SYSTEM IDENTIFICATION AND NEURAL NETWORK BASED PID CONTROL OF SERVO — HYDRAULIC VEHICLE SUSPENSION SYSTEM

O. A. Dahunsi *, J. O. Pedro† and O. T. Nyandoro‡

* *Sch. of Mechanical, Industrial and Aeronautical Engineering, University of the Witwatersrand, Private Bag 03, WITS2050, Johannesburg, South Africa. E-mail: Olurotimi.Dahunsi@students.wits.ac.za*

† *Sch. of Mechanical, Industrial and Aeronautical Engineering, University of the Witwatersrand, Private Bag 03, WITS2050, Johannesburg, South Africa. E-mail: Jimoh.Pedro@wits.ac.za*

‡ *Sch. of Electrical and information Engineering, University of the Witwatersrand, Private Bag 03, WITS2050, Johannesburg, South Africa. E-mail: Otis.Nyandoro@wits.ac.za*

Abstract: This paper presents the system identification and design of a neural network based Proportional, Integral and Derivative (PID) controller for a two degree of freedom (2DOF), quarter-car active suspension system. The controller design consists of a PID controller in a feedback loop and a neural network feedforward controller for the suspension travel to improve the vehicle ride comfort and handling quality. Nonlinear dynamics of the servo-hydraulic actuator is incorporated in the suspension model. A SISO neural network (NN) model was developed using the input-output data set obtained from the mathematical model simulation. Levenberg-Marquardt algorithm was used to train the NN model. The NN model achieved fitness values of 99.98%, 99.98% and 99.96% for sigmoidnet, wavenet and neuralnet neural network structures respectively. The proposed controller was compared with a constant gain PID controller in a suspension travel setpoint tracking in the presence of a deterministic road disturbance. The NN-based PID controller showed better performances in terms of rise times and overshoots.

Key words: Active vehicle suspension, PID, Neural network feedforward control, Servo-hydraulic actuator, Quarter-car model

1. INTRODUCTION

The design of vehicle suspension is a multidisciplinary challenge that requires compromise between complex and conflicting objectives in the face of disturbance inputs. These objectives includes: good ride comfort, good road handling, and good road holding qualities within an acceptable suspension travel range [1–3]. It is difficult to simultaneously satisfy all the design requirements for active vehicle suspension system (AVSS). Hence, a trade-off becomes necessary. Suspension travel is one of the readily measurable signal that makes the AVSS design and analysis realistic, especially within a feedback structure [4, 5].

AVSS control problem is a disturbance rejection problem, where the road roughness profile constitutes the external disturbance [3, 6]. Passive vehicle suspension remains the most popular choice for vibrations attenuation because of its simplicity and low cost. However, AVSS is the most feasible option due to its better system static stability and performance at low frequencies [3].

Numerous papers have highlighted the relative merits of semi and fully active systems [7–10]. Hrovat [6] gives a survey of applications of optimal control techniques for different types of car models, such as quarter-car, half-car, and full-car. Most of the numerical and experimental results failed to highlight the accompanying AVSS design challenges like measurement and actuator dynamic complications or the varying operating conditions of the vehicle [3, 11, 13, 14].

Controller designs based on complex multi-objective combinations like in [5] demonstrated good performance and robustness prospects. However, it is required that all the state variables be measured. This can result in a difficult to solve non-convex optimization problem.

AVSS controller designs based on linear parameter varying (LPV) control approach have been extensively applied to nonlinear models with considerations for actuator dynamics [15, 16]. However, LPV theory can only handle measurable and bounded nonlinearities [17]. LPV design is also one of the fixed-gain strategies that are designed to be optimal for nominal parameter set and specific operating condition.

The PID control is a generic control loop feedback mechanism, that remains the most industrially applied controller because of its simple structure, and the success of the Ziegler-Nichols tuning algorithms [18, 19]. Moreover, despite the straight forward Ziegler-Nichols tuning method, fine tuning of the constant gains is often done intuitively.

Previous works [11, 12] have shown that PID control possesses good prospects in terms of performance despite its disadvantages in terms of robustness, linearity and high loop gains [22–25]. This motivates for the augmentation of the PID controllers with genetic algorithm (GA) and fuzzy logic [26, 27]. The use of several evolutionary algorithms (EA) like the GA, particle swarm optimization (PSO) and differential evolution (DE) to obtain optimum PID gains has been reported in [19].

PID controller is used in this work in two forms; firstly, as a benchmark to evaluate the performance of the neural network based PID feedforward controller (PIDNN) designed for the AVSS. Secondly, as PID based controller with an overlay of NN inverse model in the feedforward mode.

It is customary in control design to use feedback as a means to stabilize unstable systems and to cut down the influence of disturbance inputs and model innacuracies. Feedforward control is known to enhance reference tracking in control designs. Control designs where feedback is used for reference tracking are usually sensitive to noise especially in systems lacking in robust properties [22].

Hagan and Demuth [28] and Cao et al. [29] highlighted various adaptive control properties of intelligent control techniques like NN, fuzzy logic, genetic algorithm and sliding mode control. NN have found wide applications in the field of control systems design because of their ability to approximate arbitrary nonlinear mapping and their highly parallel structure which allows parallel implementation, thus making it more fault-tolerant than the conventional schemes. NN also have the ability to learn and adapt on-line, and good application in multivariable systems [29–31].

The objective of system identification is to infer an approximate model of a dynamic system from its input - output data. It is desirable to seek a model with the closest representation possible especially when the system in question is nonlinear as is the case in this work. Application of NN and other intelligent techniques like fuzzy logic and genetic algorithm in system identification of nonlinear systems has been on the rise in the past two decades because of their capacity to overcome limitations encountered by the conventional methods [25, 32]

Neural network feedforward control is useful in optimizing many control problems especially in closed loop cases with stability properties. Steady-state feedforward control is not suitable for unstable systems since the control input is normally expected to be zero in steady-state systems [22].

This work aims to improve the reference tracking of the PID controller designed for the AVSS with a NN inverse model overlay in the feedforward mode. The achievement of good reference tracking through the use of feedback is usually accompanied by high sensitivity to noise. Thus in a situation where good controller performance has been achieved using feedback control, it is desirable to provide a guarantee for reduced sensitivity to noise through the addition of a suitable control technique in the feedforward mode [22].

The paper is organised as follows: The 2DOF, quarter-car AVSS model is described in Section 2. Section 3 describes the performance specifications, system identification process and controller design. Numerical simulation and discussion of results are presented in Section 4 before concluding the paper in Section 5.

2. SYSTEM MODELLING

2.1 Physical Modelling

The 2DOF, quarter-car AVSS is modelled as a dynamic system that consists of sprung mass m_s, and unsprung mass m_u. The masses are interconnected by nonlinear spring k_s, damper b_s and hydraulic actuator F, as shown in Figure 1, and k_t is the spring constant due to the compressibility of the pneumatic tyre. The vertical displacement of the car

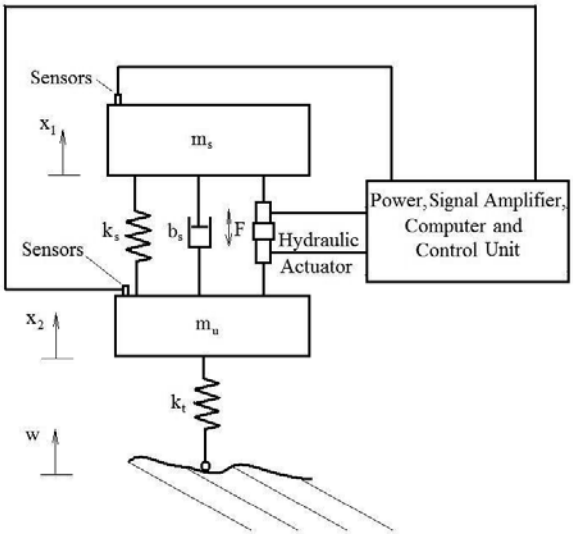

Figure 1: Simplified quarter car model

body, wheel and the road disturbance are represented by x_1, x_2 and w respectively. The hydraulic actuator force F is applied between the sprung and unsprung masses. The relative displacement between the vehicle body and the wheel $(x_2 - x_1)$, represents the suspension travel and the relative displacement between the wheel and the road $(x_2 - w)$, characterizes the road holding quality.

2.2 Mathematical Modelling

Application of Newton's law to the quarter car model shown in Figure 1 yields the governing equations in the state space form [15, 16, 33]:

$$\dot{\mathbf{x}} = \mathbf{f}(\mathbf{x}, \mathbf{w}) + \mathbf{g}(\mathbf{x})\,\mathbf{u}; \tag{1}$$

$$y = h(x) = y_1 = x_2 - x_1 \tag{2}$$

where:

$$\mathbf{f}(\mathbf{x},\mathbf{w}) = \begin{bmatrix} f_1 & f_2 & f_3 & f_4 & f_5 & f_6 \end{bmatrix}^{\mathbf{T}}, \tag{3}$$

$$\mathbf{g}(\mathbf{x}) = \begin{bmatrix} 0 & 0 & 0 & 0 & 0 & \frac{1}{\tau} \end{bmatrix}^{\mathbf{T}} \tag{4}$$

The state vector is

$$\mathbf{x} = \begin{bmatrix} x_1 & x_2 & x_3 & x_4 & x_5 & x_6 \end{bmatrix}^{\mathbf{T}} \tag{5}$$

and the control input is u.

$$f_1 = x_3 \tag{6}$$

$$f_2 = x_4 \tag{7}$$

$$f_3 = \frac{1}{m_s}\Big\{k_s^l(x_2-x_1)+k_s^{nl}(x_2-x_1)^3+b_s^l(x_4-x_3) - b_s^{sym}|x_4-x_3|+b_s^{nl}\sqrt{|x_4-x_3|}sgn(x_4-x_3) - Ax_5\Big\} \tag{8}$$

$$f_4 = \frac{1}{m_u}\Big\{-k_s^l(x_2-x_1)-k_s^{nl}(x_2-x_1)^3-b_s^l(x_4-x_3) + b_s^{sym}|x_4-x_3|-b_s^{nl}\sqrt{|x_4-x_3|}sgn(x_4-x_3) - k_t(x_2-w)+Ax_5\Big\} \tag{9}$$

$$f_5 = \gamma\Phi x_6 - \beta x_5 + \alpha A(x_3-x_4) \tag{10}$$

$$f_6 = \frac{-x_6}{\tau} \tag{11}$$

where; $\Phi = \phi_1 + \phi_2$, $\phi_1 = sgn[P_s - sgn(x_6)x_5]$, $\phi_2 = \sqrt{|P_s - sgn(x_6)x_5|}$, $\alpha = \frac{4\beta_e}{V_t}$, $\beta = \alpha C_{tp}$, and $\gamma = C_d S\sqrt{\frac{1}{\rho}}$. A is the area of the piston, x_3 and x_4 are the vertical velocities of the sprung and unsprung masses respectively, x_5 is the pressure drop across the piston, x_6 is the servo valve displacement, P_s is the supply pressure going into the cylinder and P_r is the return pressure going out of the cylinder. P_u is the oil pressure in the upper portion of the cylinder and P_l is the oil pressure in the lower portion of the cylinder. V_t is the total actuator volume, β_e is the effective bulk modulus of the system, Φ is the hydraulic load flow, C_{tp} is the total leakage coefficient of the piston, C_d is the discharge coefficient, S is the spool valve area gradient and ρ is the hydraulic fluid density.

The spring and damping forces have linear and nonlinear components. Spring constant k_s^l and damping coefficient b_s^l affects the spring force and damping force in the linear region. b_s^{sym} contributes an asymmetric characteristics to the overall behaviour of the damper. k_s^{nl} and b_s^{nl} are responsible for the nonlinear components of the spring and damper forces respectively.

Figure 2 illustrates the hydraulic actuator mounted in between the sprung and unsprung masses. Q_u and Q_l are the hydraulic fluid flow rates into the upper and the lower chambers of the hydraulic cylinder respectively.

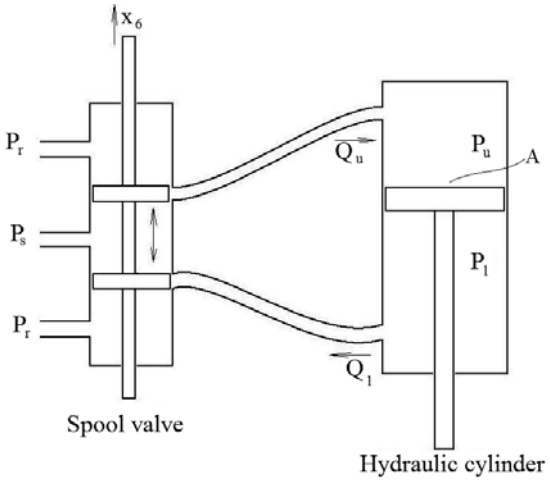

Figure 2: Schematic of the double acting hydraulic strut

The actuator is controlled by means of electro-hydraulic servo-valves in a three land four-way spool valve system. The maximum control input (voltage) of $10V$ was applied to the servo-valves to achieve a maximum suspension travel of $10cm$.

The deterministic road disturbance used in Equation 9 is given by:

$$w(t) = \begin{cases} \frac{a}{2}(1-cos\frac{2\pi Vt}{\lambda}) & 1.25 \le t \le 1.5 \\ 0 & \text{otherwise} \end{cases} \tag{12}$$

where a is the bump height, V is the vehicle speed and λ is the half wavelength of the sinusoidal road undulation. Figure 3 shows the road disturbance profile.

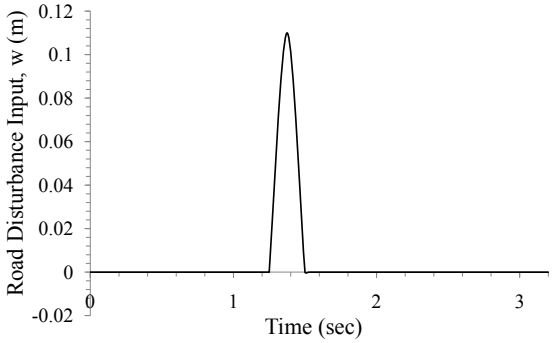

Figure 3: Road profile

The values of the system parameters used in the modelling are given in Table 1:

3. CONTROLLER DESIGN

The controller design is based on the indirect adaptive control approach, using PID feedback control that is complemented by feedforward generated by an inverse neural network model. The NN-based controller implementation requires the following two steps: system

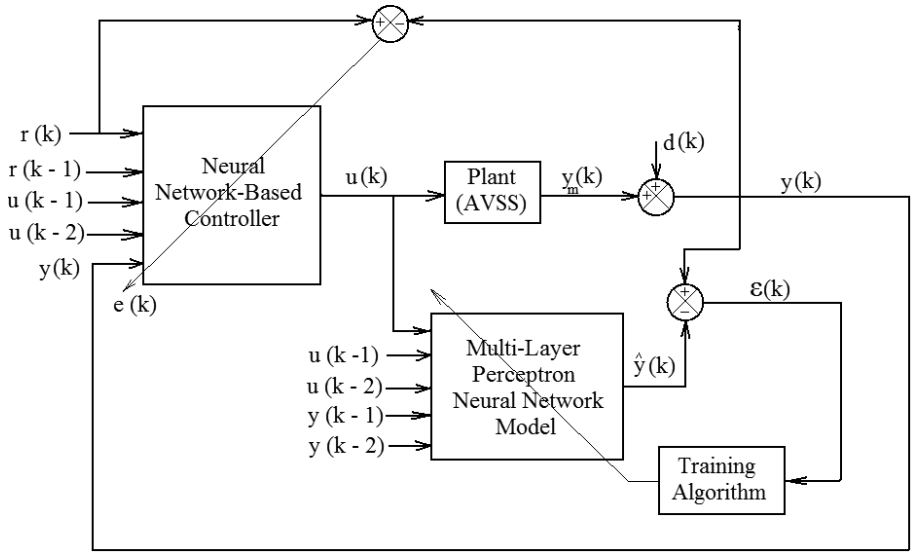

Figure 4: Architecture for Neural Network based System Identification and Control

Table 1: Parameters of the Quarter-Car Model [15, 16]

Parameters	Value
sprung mass (m_s)	290kg
unsprung mass (m_u)	40kg
suspension stiffness (k_s^l)	$2.35*10^4 N/m$,
suspension stiffness (k_s^{nl})	$2.35*10^6 N/m$
tyre stiffness (k_t)	$1.9*10^5 N/m$
suspension damping (b_s^l)	$700 Ns/m$
suspension damping (b_s^{nl})	$400 Ns/m$
suspension damping (b_s^{sym})	$400 Ns/m$
actuator parameter (α)	$4.515*10^{13}$
actuator parameter (β)	1
actuator parameter (γ)	$1.545*10^9$
piston area (A)	$3.35*10^{-4} m^2$
supply pressure (P_s)	$10,342,500 Pa$
time constant (τ)	$3.33*10^{-2} sec$
bump height (a)	$0.11m$
vehicle speed (V)	$30 ms^{-1}$
disturbance half wavelength (λ)	$7.5m$

identification and controller design.

In order to design a NN-based controller, it is essential to first obtain an accurate dynamic model, through system identification, as a representation of the actual system. Figure 4 shows the schematic architecture for system identification and controller design of the system, where $\hat{y}(k)$ is the identified model output, $d(k)$ is the disturbance signal, $\varepsilon(k) = y(k) - \hat{y}(k)$ the error signal, $y(k)$ is the controlled output, $u(k)$ is the control input, and $e(k) = r(k) - y(k)$.

The main goal of the controller is to track a generated desired suspension travel in the presence of the deterministic road disturbance (Equation 12). The controller should satisfy the following requirements:

1. Nominal stability: The closed loop should be nominally stable.
2. Good command following: The controller should be able to track a square wave reference trajectory with rise time not greater than $0.1 sec$, maximum overshoot not greater than 5% and without steady state error.
3. Disturbance rejection: The controller should demonstrate good low frequency disturbance attenuation.
4. Performance index: The controller should minimize the performance index given by:

$$J = \frac{1}{t_f}\int_0^{t_f}\left[\left(\frac{y(t)-y_{ref}(t)}{y_{max}}\right)^2 + \left(\frac{u(t)}{u_{max}}\right)^2\right]dt \quad (13)$$

where t_f is the final time (which in this case is $5 sec$), y_{ref} is the desired suspension travel, y_{max} is the the maximum allowable value of the suspension travel (controlled output), and u_{max} is the maximum allowable value of the supply voltage (control input).

3.1 Nonlinear System Identification

System identification stage is a function approximation process where the dynamic model of the system is established based on observed input-output data. Feedforward, multilayer perceptron (MLP), error back propagation neural network is used here for the system identification. This is due to its simplicity and ability to learn nonlinear relations from a set of input-output data [22].

Training inputs are supplied to the input layer of the network in a forward sweep such that the output of each

element is computed layer by layer. Backpropagation training is a process of training the network with the input and target vectors until it can associate input vectors with appropriate output vectors [34].

In this work, the suitability of the neural network in developing dynamic models that is representative of the actual nonlinear plants based on the interactions between the inputs and outputs is exploited. The identification process consists of the four steps shown in Figure 5: experimentation, model structure selection, model estimation and model validation [22]. Control design stage comes after the system identification, here the NN plant model is used to design the controller.

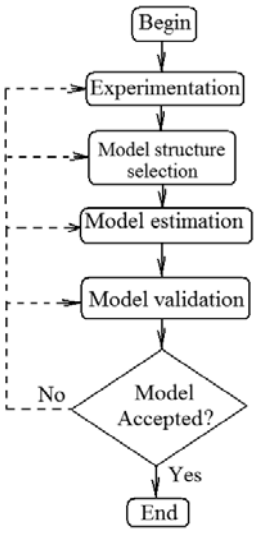

Figure 5: Flowchart form of system modelling procedure

The objective of the identification process is to minimize the error signal $\varepsilon(k) = y(k) - \hat{y}(k)$, where k = 1,.....,N (see Figure 6). The NN parameters in the identification model are adjusted in an increasing manner until the training data satisfies the desired performance criteria, which in this case is the sum of the mean square error (MSE) [25,34,35]:

$$MSE = \gamma \frac{1}{N} \sum_{k=1}^{N} [y(k) - \hat{y}(k)]^2 = \gamma \frac{1}{N} \sum_{k=1}^{N} \varepsilon^2(k) \qquad (14)$$

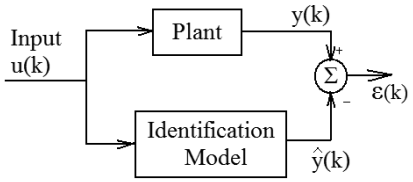

Figure 6: Basic system identification structure

where γ is the performance ratio. The choice of the performance ratio must be considered with caution since it represents the relative weight between the mean square errors and the mean square network parameters (that is, weights and biases). The choice of γ may influence the smoothness of the network response. The sampling time is chosen in accordance with the fastest dynamics of the system [22, 33].

Experimentation:

The AVSS is identified from a set of input-output data pairs collected from numerical experiments. These are given in form of the AVSS model Equations (1) - (6) simulations and collected in the form:

$$Z^N = f[u(k), y(k)]; \quad k = 1, ..., N \qquad (15)$$

where Z^N is the input-output data set, $u(k)$ is the input signal, $y(k)$ is the output signal, k is the sampling instant, and N is the total number of samples. The input-output data was collected using the structure illustrated by Figure 7:

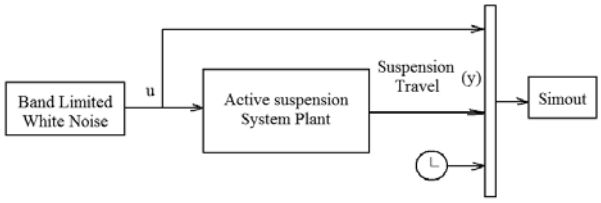

Figure 7: Structure input-output data collection

The AVSS plant model identification was conducted using a 20,000 input-output data pairs - divided into two equal parts for training and validation as shown in Figures 8 and 9. A non-saturating "band-limited white noise" random input was used to excite the AVSS plant in its operating range, $u(k) \in [-10V, +10V]$. The sampling interval of $0.001sec$ was chosen in accordance with the fastest dynamic of the system [22, 33].

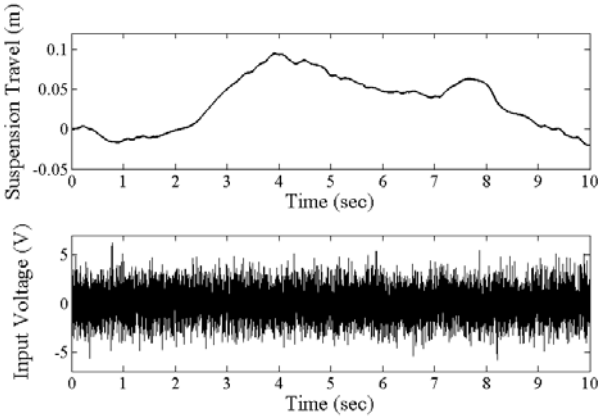

Figure 8: Estimation (training) data set

Model Structure Selection:

The Neural Network AutoRegressive eXogenous inputs (NNARX) model has been proven to readily represent any nonlinear, discrete, time-invariant system. It is preferable

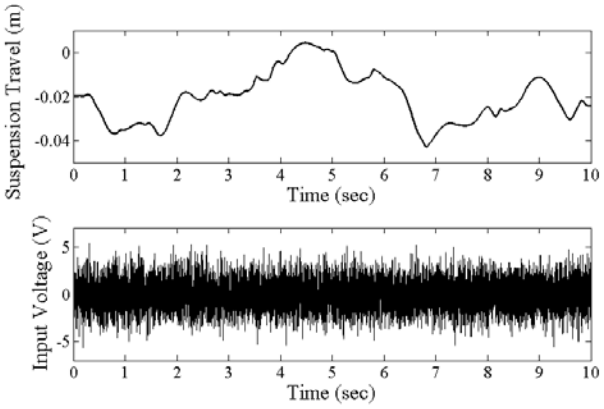

Figure 9: Validation data set

when the system order is high, however, increasing its order could affect some dynamic characteristics like stability. It is also simpler, non-recursive (unlike nonlinear models based output error (OE) and Auto Regressive Moving Average with eXogenous inputs (ARMAX), wherein future inputs depend on present and future outputs) and more stable since it requires no feedback [20,22,36]. The general structure of the NNARX is shown in Figures 10 and 11.

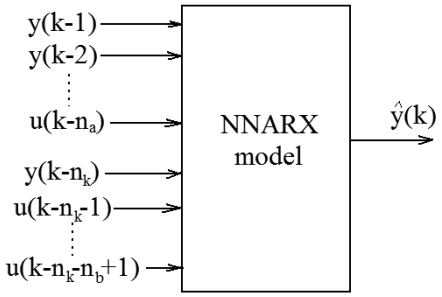

Figure 10: NNARX model structure

The AVSS nonlinear system can be represented by NNARX model structure for a finite number of past inputs $u(k)$ and outputs $y(k)$ [20,25,37,38]:

$$y(k) = f[\phi(k), \theta] + \vartheta(k) \tag{16}$$

As a result of the numerical experiment and training, the network implements an estimation of the nonlinear transformation, $\hat{f}(*)$ which leads to the predicted output. The one-step ahead prediction (1-SAP) based on the identification structure is given by:

$$\hat{y}(k) = f[\phi(k), \theta] \tag{17}$$

and the regression vector is

$$\begin{aligned} \phi(k) \quad = \quad & [y(k-1), y(k-2), \ldots, y(k-n_a), u(k-n_k), \\ & u(k-n_k-1), \ldots, u(k-n_k-n_b+1)) \end{aligned}$$

where f is the nonlinear function that is realized by the

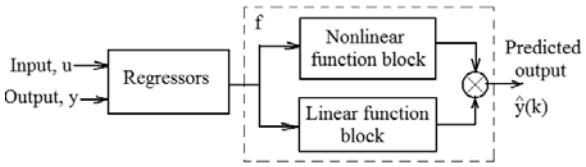

Figure 11: Neural network nonlinear ARX Structure

neural network model, $\phi(k)$ represents the regressors, vector θ contains the adjustable weights, $\vartheta(k)$ represents the model residual, n_k delay from input to the output in terms of number of samples, and n_a and n_b make up the order of the system which is the number of output and inputs used to predict the new output. Lipschitz algorithm was used to the determine the system lag (see Figures 12 and 13). The figures present the plot of the order index based on the evaluated Lipschitz quotients for the input - output pair combinations against the lag space (number of past inputs and outputs) ranging from 1 to 10.

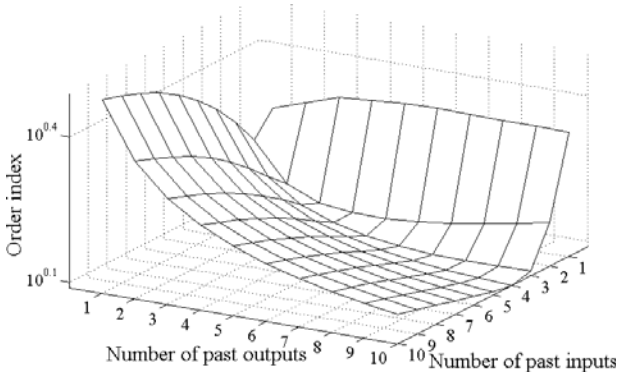

Figure 12: Model order determination by lag-space method

Figure 13 shows that the slope of the graph decreases when the model order is ≥ 2, thus defining the "knee point" of the curve. This leads to the choice of two as the number of past inputs and outputs respectively; and the number of neurons in the hidden layer becomes five since the time delay is one [22,25]. The choice of a model order higher than two may result in data overfitting with lower MSE.

Model Estimation:

The neural network structures are selected for use in the network training of the model. Simplicity of the NN structure and computational ease are two guiding factors considered in the model estimation process. Thus a feedforward multilayer perceptron neural network (MLPNN) structure that contains: an input layer, a hidden layer and an output layer shown in Figure 14 was developed. The parameters for training of the neural network model are listed in Table 2.

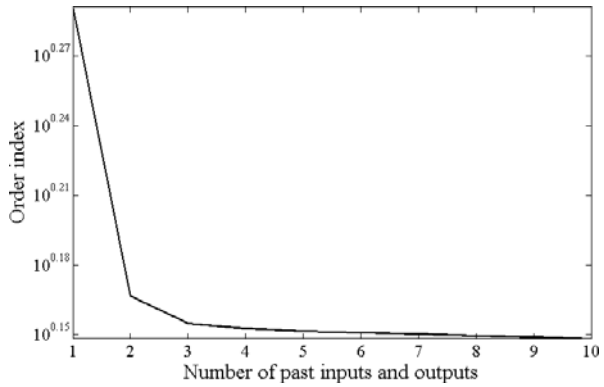

Figure 13: Two dimensional view of the order of index versus lag - space

Levenberg-Marquardt minimization algorithm was used to train the network due to its rapid convergence and robustness. The input layer contains two neurons and a bias, the hidden layer contains five neurons with tangent hyperbolic activation function:

$$f(x) = tanh(x) = \frac{e^x - e^{-x}}{e^x + e^{-x}} \tag{18}$$

while the output layer contains one neuron with linear

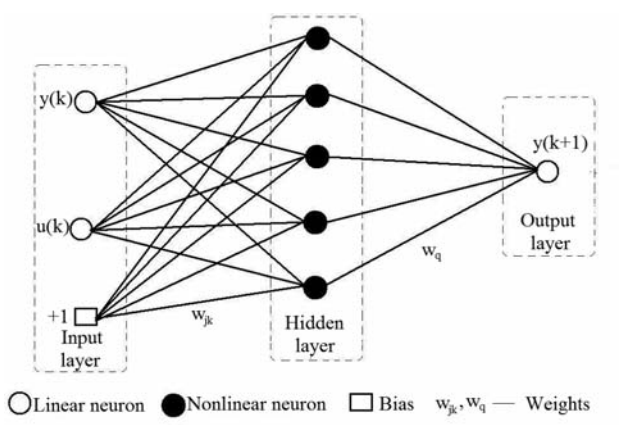

Figure 14: Neural network layer structure

activation function [21, 22, 39].

The choice of Levenberg-Marquardt training algorithm is motivated by the results shown in Table 3. It has the least mean square error (MSE) using the maximum number of available epochs (300). Levenberg-Marquardt training algorithm is also preferred to the other algorithms because it improves over time relative to the other algorithms and it is a compromise between the gradient descent and Newton optimization methods [22, 34, 40].

Model Validation:

The performance of the trained network as based on the validation data is shown in Figure 15 where the quality of the identification is indicated by the mean square error, which is of the order of 10^{-11}.

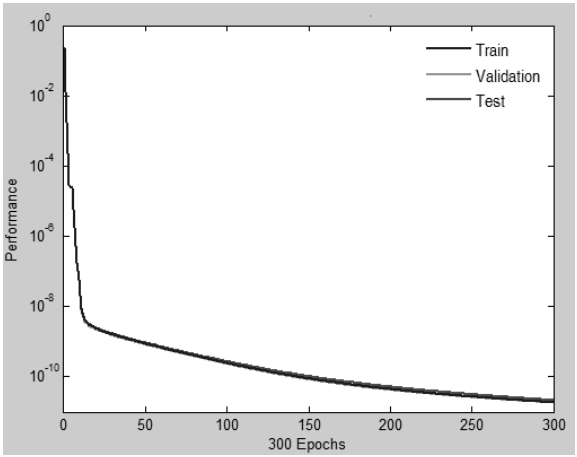

Figure 15: Neural network training performance

Figure 16 presents the fitness analysis of three one-step ahead predictions for sigmoidnet, wavenet and neuralnet structures to the validation data. The fitness values for each structures were 99.98%, 99.98% and 99.96% respectively.

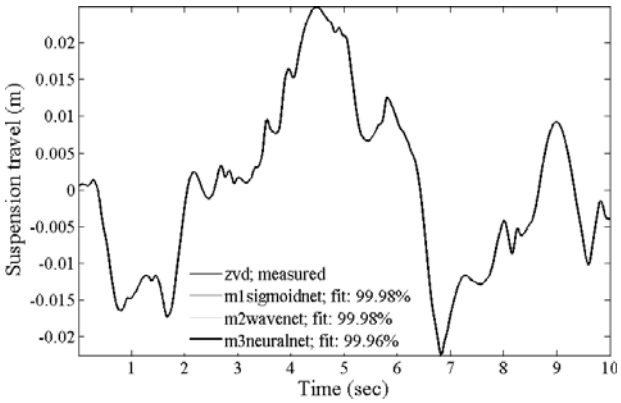

Figure 16: Fitness analysis for one-step ahead predictions based on sigmoidnet, wavenet and neuralnet structures

In Figure 17 the residuals were found to be of the order of 10^{-8}. Figure 18 shows a relatively steady auto-correlation trend of the residuals and about 90% of the points for cross-correlation between the input signal and the residuals of the output (suspension travel) falls within the 95% confidence interval. The validity of the model is further demonstrated by the low mean square error value $(1.84492 * 10^{-11})$ in Figure 15, high percentage fitness values in Figure 16 and low order of the residuals in Figure 17.

Table 2: Parameters for the Neural Network Model

Parameters	Value	Parameters	Value
Total number of samples	500 (control)	Total sampling time	5sec
Number of training epochs	300	Number of iterations	10,000
		Time delay	1
Training algorithm	Levenberg-Marquardt algorithm	Number of hidden layer neurons	5
Number of layers	2	sampling time, T_s	0.001sec
Number of past outputs	2	Number past inputs	2

Table 3: Performance of Neural Network Training Functions

	Algorithm	Number of Epochs used out of 300	Mean Square Error
1	BFGS quasi-Newton backpropagation	75	$3.15857 * 10^{-6}$
2	Powell-Beale conjugate gradient backpropagation	13	$1.46828 * 10^{-4}$
3	Fletcher-Powell conjugate gradient backpropagation	188	$4.95962 * 10^{-6}$
4	Polak-Ribiere conjugate gradient backpropagation	68	$7.3317 * 10^{-6}$
5	Gradient descent backpropagation	300	$9.50216 * 10^{-3}$
6	Gradient descent with momentum and adaptive backpropagation	300	$1.00666 * 10^{-2}$
7	Gradient descent with adaptive learning backpropagation	243	$5.07354 * 10^{-4}$
8	Gradient descent with momentum and adaptive backpropagation	159	$1.19449 * 10^{-4}$
9	Levenberg-Marquardt backpropagation	300	$1.84492 * 10^{-11}$
10	One step secant backpropagation	90	$5.81278 * 10^{-6}$
11	Resilient backpropagation	300	$7.87337 * 10^{-6}$
12	Scaled conjugate gradient backpropagation	52	$1.4651 * 10^{-5}$

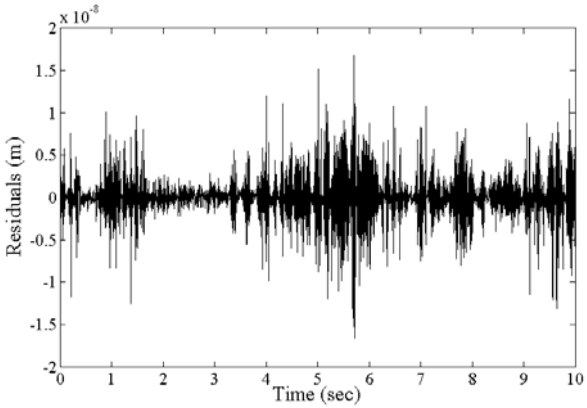

Figure 17: Model residuals

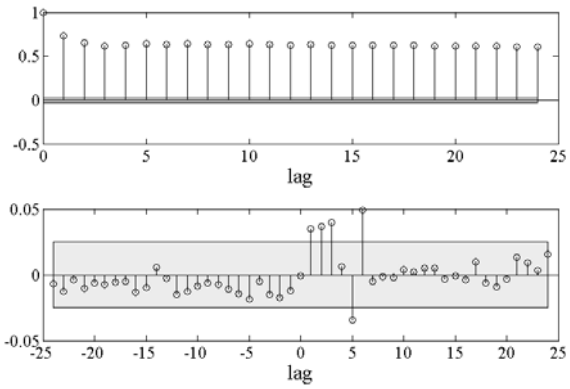

Figure 18: Auto and Cross Correlation Analysis

3.2 PID Control and Tuning

The structure of the PID controller is given as [22, 42]:

$$U(s) = \left(K_p \frac{1 + T_i s}{T_i s} \frac{1 + T_d s}{1 + \alpha T_d s} \right) E(s) \qquad (19)$$

where $E(s) = Y_{ref}(s) - Y(s)$ is the error signal, $Y_{ref}(s)$ is the reference signal, $Y(s)$ is the actual output signal, $U(s)$ is the plant input signal, K_p is the proportional gain, T_d is the derivative time constant, T_i is the integral time constant and α is the lag factor in the derivative component of the PID controller.

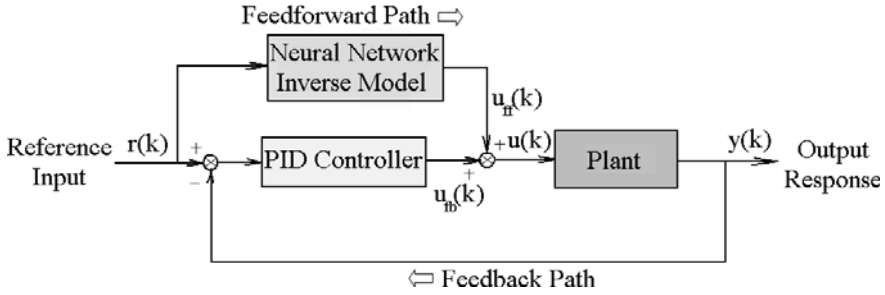

Figure 19: PID Feedback Scheme being Optimised with a Neural Network Inverse Model

Table 4: PIDNN and PID tuning parameters used

Parameters	PIDNN Tuning Values	PID Tuning Values
Proportional gain, K_p	6.5	3.0
Integral time, T_i	0.0238	0.0667
Derivative time, T_d	0.4041	0.04035
Lag factor, α	0.0147	0.047

Ziegler-Nichols tuning rule is used with a decay ratio of 0.25 to obtain the PID controller gains. PID controllers are known to often generate high control inputs which can lead to saturation. Thus, efforts were made during tuning to ensure that the control input was within the stipulated range. The tuning parameters are presented in Table 4.

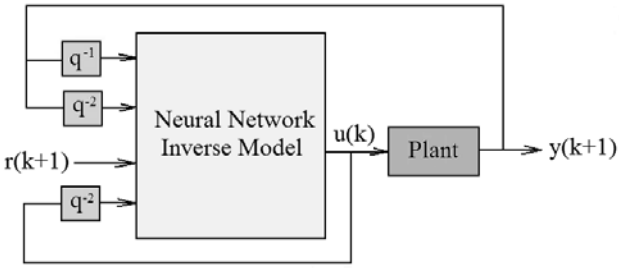

Figure 20: Direct Inverse Control

3.3 Neural Network Based Feedforward Control

The control structure in Figure 19 presents an arrangement for a PID control feedback overlaid with a neural network (PIDNN) inverse model. The essence of the neural network inverse model is to optimise the performance of the PID controller based on the principle of additive feedforward. This method is one of the direct control design of the neural network based control. It is sometimes useful in regulation problems where the reference attains constant levels for longer periods of time, it helps in speeding up the tracking of set points changes [22].

The inverse model is illustrated in Figure 20. The training of a network as an inverse of a system requires the application of the system identification procedure illustrated by Figure 5 but it is done off-line.
Moreover, the difference of the inverse NN model is in the choice of the regressors and network output. The inverse model is here applied to AVSS plant by inserting the desired output, reference $r(k+1)$, instead of the system output $y(k+1)$, which is an unknown value, at the input point of the inverse model, this training is implemented in the form shown in Equation 21. If the AVSS is described by [22, 41]:

$$y(k+1) = g[y(k),\ldots,y(k-n_a+1,u(k),\ldots,u(k-n_b)] \tag{20}$$

then the desired network is the one that isolates the latest control input, $u(k)$ given by

$$\begin{aligned}\hat{u}(k) &= \hat{g}^{-1}[r(k+1),y(k),\ldots,y(k-n_a+1,\\ &\quad u(k),\ldots,u(k-n_b)]\end{aligned} \tag{21}$$

the network is then trained to minimize the criterion

$$J(\theta,Z^N) = \frac{1}{2N}\sum_{k=1}^{N}[u(k)-\hat{u}(k|\theta)]^2 \tag{22}$$

The system outputs are substituted with the corresponding feedforward component of the control input given by

$$\begin{aligned}u_{ff}(k) &= \hat{g}[r(k-1),\ldots,r(k-n_a+1,\\ &\quad u_{ff}(k-1),\ldots,u_{ff}(k-n_b)]\end{aligned} \tag{23}$$

this can then be used to drive the system output at $k+1$ to reference $r(k+1)$ as shown in Figures 4 and 20.

The network is trained by invoking Levenberg-Marquardt training algorithm (system identification). This was done off-line by minimizing the criterion $J(\theta,Z^N)$ where θ specifies the weights of the network. Ziegler-Nichol's tuning rule, with a decay ratio of 0.25, is used to obtain the tuning parameters for the PIDNN as presented in Table 4.

4. RESULTS AND DISCUSSION

The physical model which is represented by Figure 1 has been modelled mathematically in the state-space form given by Equations 1-11. Numerical experimentation based on the mathematical model yielded a NN model of the plant that was used in the controller design.

The PIDNN and PID controller were applied to an AVSS nonlinear model with actuation force generated by an electro-hydraulic actuator. A variable but preset control input in the form of voltage (which was ≤ 10V) was supplied to the servo-valve to generate the actuation force at the piston. The control problem given by Equation 1 is to obtain a control input, $u(t)$ that follows a reference trajectory $y(t)$ while minimizing the performance criterion (Equation 13). Meanwhile, the reciprocals of the squared values of y_{max} and u_{max} gives the values of the weighting factors that was used in the computation of the performance index.

The identification and control processes were implemented in MATLAB using the MATLAB system identification toolbox and neural network based control system design (NNCNTRL20) toolboxes. The parameters used for the simulations are given in Tables 1, 2 and 4.

Figures 21 and 22 present the command tracking of both controllers.The PIDNN tracking is characterized by the presence of marginal steady state error and overshoots that diminished with time, but the trajectory tracking of the PID appear better though its overshoots at the points of transition is a regular feature. The maximum overshoot measured for the PIDNN is just marginally greater than overshoot in the PID control, but the maximum overshoots for both controller exceed the specified values.

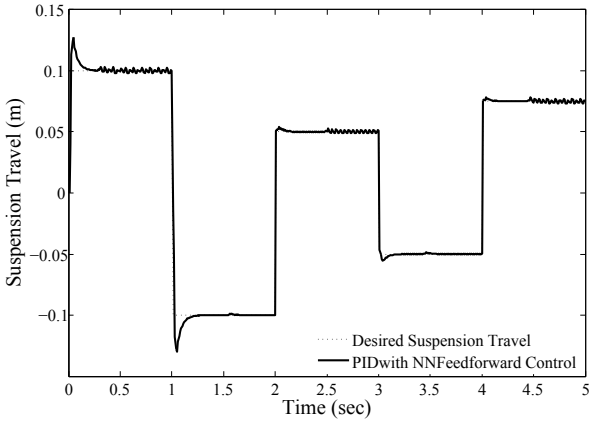

Figure 21: Suspension travel reference tracking using the NN based PID controller

Both controllers have rise times that are below the specified value for design but the rise time for PIDNN is $0.004sec$ lower than that for the PID controller. The PIDNN controller could not also reach the zero steady state error like the PID because of the oscilations that occur just before the transition point.

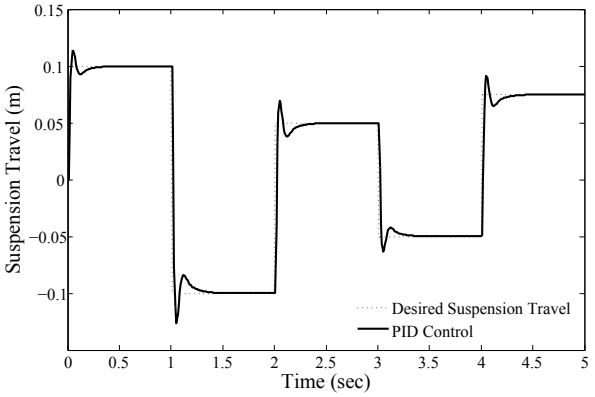

Figure 22: Suspension travel reference tracking using the PID controller

Figures 23 and 24 show the cost of achieving the performance of the PIDNN controller summarised in Table 5 in terms of the supplied voltage to the servo valve of the actuator as control input. The supply voltage to the PIDNN was characterized by continuous chattering and it exceeded the required supply voltage value in four instances. The maximum range of the supply voltage to the PID controller is $-4.2V - 3.3V$. The PID supply voltage is also characterized by spikes at the transition points.

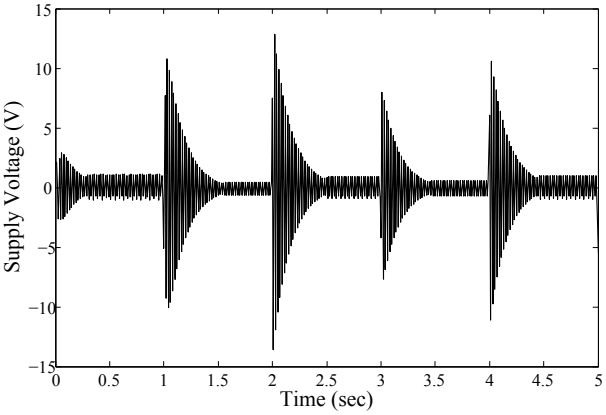

Figure 23: NN based PID control input

Complete minimization of the performance criterion could not be achieved by both controllers but the performance index of the PID is twice better than the performance index of the PIDNN controller. This performance criterion has put into consideration the sum of square of the weighted controlled output error and the control input.

Considering the values for all the performance evaluation parameters listed in Table 5, the overall superior performance of the PID controller is evident but from Figure 25, the performances of the PID controller at the transitional points are not as physically realisable as the PIDNN. While the PIDNN gradually returns to zero, the PID controller shoots to higher performance index at these

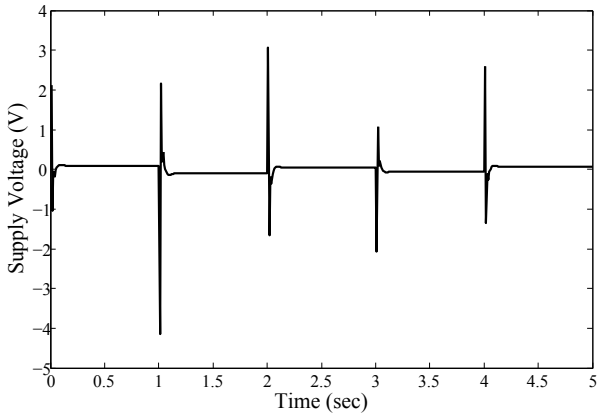

Figure 24: PID control input

points and returns to zero immediately.

Table 5: Evaluation of the controller performances

Performance parameters	Specified values	PIDNN	PID
Maximum overshoot	$\leq 5\%$	27.7%	26.1%
Rise time, *sec*	$\leq 0.1\%$	0.014	0.018
Steady state error	0%	4%	0%
Control input, V	± 10	136%	42%
Performance index, J	0	0.057	0.025

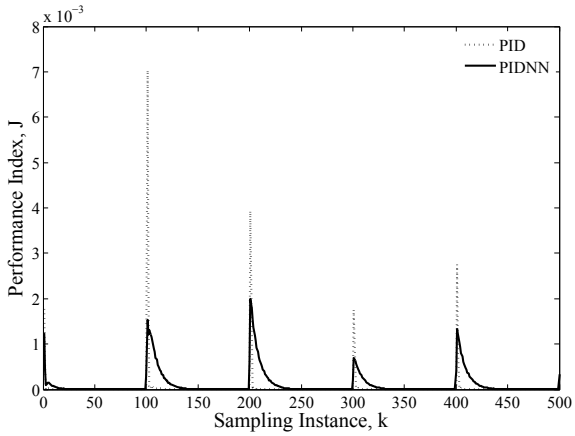

Figure 25: Comparison of Performance Indices at all the Sampling Instances

5. CONCLUSION

A PID controller with a neural network feedforward control has been designed for a nonlinear AVSS. The system identification process to obtain an inverse NN model for the controller design was achieved at an average fitness value of 99.98% and prediction error with order of 10^{-8}.

Both controllers were able to track the reference well though with overshoots and both controllers had rise time values that were less than the required. The supply voltage to the PIDNN exceeded the limits at four instance while the PID controller was always lower than the supply voltage limit by at least 50%.

The performance index for the PID controller was twice lower than the index for the PIDNN but examination of the performance indices at each sampling instances showed that, although the PID controller had better performance than the PIDNN, it is less physically realisable than the PIDNN control.

The choice of PIDNN over the conventional PID control is due to drawbacks like the nonlinear nature of AVSS and its susceptibility to parameter and disturbance variation, often PID controller design fail to guarantee robustness and model uncertainty.

REFERENCES

[1] H. Du and N. Zhang: "H_∞ Control of Active Vehicle Suspensions with Actuator Time Delay", *Journal of Sound and Vibration*, Vol. 301, No. 1-2, pp. 236-252, March 2007.

[2] M. S. Kumar and S. Vijayarangan: "Analytical and Experimental Studies on Active Suspension System of Light Passenger Vehicle to Improve Ride Comfort", *Mechanika*, Vol. 65, No. 3, pp. 34-41, June 2007.

[3] J. O. Pedro: "H_2 - LQG/LTR Controller Design for Active Suspension Systems",*R and D Journal of the South African Institution of Mechanical Engineering*, Vol. 23, No. 2, pp. 32-41, November 2007.

[4] B. Gao, D. G. Tilley, R. A. Williams, A. Bean and J. Donahue: "Control of Hydropneumatic Active Suspesion based a nonlinear Quarter-Car Model",*Proceedings of the Institute of Mechanical Engineers, Part I*, Vol. 220, No. 1, pp. 75-81, January 2006.

[5] H. Du and N. Zhang: "Designing H_∞/GH_2 Static - Output Feedback Controller for Vehicle Suspensions Using Linear Matrix Inequalities and Genetic Algorithms", *Vehicle Systems Dynamics*, Vol. 46, No. 5, pp. 385-412, May 2008.

[6] D. Hrovat: "Survey of Advanced Suspension Developments and Related Optimal Control Applications", *Automatica*, Vol. 33, No. 10, pp. 1781-1817, October 1997.

[7] M. K. Ghosh and R. Dinavahi: "Vibration Analysis of a Vehicle System Supported on a Damper-Controlled Variable-Spring-Stiffness Suspension", *Proceedings of the Institute of Mechanical Engineers, Part D*, Vol. 219, No. 5, pp. 607-619, May 2005.

[8] I. Ballo: "Comparison of the Properties of an Active and Semi-Active Suspension", *Vehicle System Dynamics*, Vol. 45, No. 11, pp. 1065-1073, November 2007.

[9] J. Renn and T. Wu: "Modelling and Control of a new $\frac{1}{4}T$ Servo-Hydraulic Vehicle Active Suspension System", *Journal of Marine Science and Technology*, Vol. 15, No. 3, pp. 265-272, September 2007.

[10] M. Biglarbegian, W. Melek and F. Golnaraghi: "A Novel Neuro-Fuzzy Controller to Enhance the Performance of Vehicle Semi-Active Suspension Systems", *Vehicle System Dynamics*, Vol. 46, No. 8, pp. 691-711, August 2008.

[11] O. A. Dahunsi, J. O. Pedro and O. T. Nyandoro: "Neural Network-Based Model Predictive Control of a Servo-Hydraulic Vehicle Suspension System", *Proceedings of the 2009 IEEE Africon*, Nairobi, Kenya, September 2009.

[12] O. A. Dahunsi, J. O. Pedro and O. T. Nyandoro: "Neural Network-Based PID Control of a Servo-Hydraulic Vehicle Suspension System", *Proceedings of the Seventh South African Conference on Computational and Applied Mechanics (SACAM10)*, University of Pretoria, South Africa, January 2010.

[13] S. Chantranuwathana and H. Peng: "Adaptive Robust Force Control for Vehicle Active Suspension", *International Journal of Adaptive Control and Signal Processing*, Vol. 18, No. 2, pp. 83 - 102, March 2004.

[14] X. Shen and H. Peng: "Analysis of Active Suspension Systems with Hydraulic Actuators", *Proceedings of the 2003 IAVSD Conference*, Atsuigi, Japan, pp. 1-10, August 2003.

[15] I. Fiahlo and G. J. Balas: "Road Adaptive Active Suspension using Linear Parameter-Varying Gain-Scheduling", *IEEE Transactions on Control Systems Technology*, Vol. 10, No. 1, pp. 43-54, January 2002.

[16] P. Gaspar, I. Szaszi and J. Bokor: "Active Suspension Design Using Linear Parameter Varying Control", *International Journal of Autonomous Systems (IJVAS)*, Vol.1, No. 2, pp. 206 - 221, June 2003.

[17] C. Poussot-Vassal, O. Sename, L. Dugard, P. Gaspar, Z. Szabo and J. Bokor: "Multi-objective qLPV H_∞/H_2 Control of a Half Vehicle", *Proceedings of the 10th MINI Conference on Vehicle System Dynamics, Identification and Anomalies*, Budapest, Hungary, November 2006.

[18] J. G. Juang, M. T. Huang and W. K. Liu: "PID Control Using Presearched Genetic Algorithms for a MIMO System", *IEEE Transactions on Systems, Man, and Cybernetics-part C:Applications and Reviews*, Vol. 38, No. 5, pp. 716 - 727, September 2008.

[19] M. W. Iruthayarajan and S. Baskar: "Evolutionary Algorithms Based Design of Multivariable PID Controller", *Expert Systems with Applications*, Vol. 36, No. 5, pp. 9159 - 9167, July 2009.

[20] J. D. Bomberger and D. E. Seborg: "Determination of Model Order for NARX Models Directly from Input - Output Data", *Journal of Process Control*, Vol. 8, No. 5, pp. 459 - 468, October 2009.

[21] M. Norgaard: "Neural Networks Based Control System Design", *Tech.Report 00-E-892*, Department of Automation, Technical University of Denmark, 2000.

[22] M. Norgaard, O. Ravn, N. K. Poulsen and L. K. Hansen: "Neural Networks for Modelling and Control of Dynamic Systems: A Practitioner's Handbook", *Springer*, Boston, MA, 2000.

[23] Z. Gao: "From Linear to nonlinear Control Means: A Practical Progression", *ISA Transactions*, Vol. 41, No. 2, pp. 177-189, April 2002.

[24] A. Herreros, E. Baeyens and J. R. Peran: "Design of PID - type Controllers Using Multiobjective Genetic Algorithms", *ISA Transactions*, Vol. 41, No. 4, pp. 457 - 472, October 2002.

[25] N. Kishor, R. P. Saini and S. P. Singh: "Small Hydro Power Plant Identification Using NNARX Structure", *Neural Computing and Applications*, Vol. 14, No. 3, pp. 212 - 222, September 2005.

[26] J. Z. Feng, J. Li and F. Yu: "GA-Based PID and Fuzzy Logic Control for Active Vehicle Suspension System", *International Journal of Automotive Technology*, Vol. 4, No. 4, pp. 181- 191, December 2003.

[27] Y. Kuo and T. S. Li: "GA-Based Fuzzy PI/PD Controller for Automotive Active Suspension System", *IEEE Transactions on Industrial Electronics*, Vol. 46, No. 6, pp. 1051 - 1056, December 1999.

[28] M. T. Hagan and H. B. Demuth: "Neural Networks for Control", *American Control Conference*, Invited Tutorial for American Control Conference 1999, pp. 1642 - 1656, San Diego, USA June 1999.

[29] J. Cao, H. Liu, P. Li and D. Brown: "State of the Art in Vehicle Active Suspension Adaptive Control Systems based on Intelligent Methodologies", *IEEE Transactions of Intelligent Transportation Systems*, Vol. 9, No. 3, pp. 392 - 405, September 2008.

[30] Y. Jin and D. J. Yu: "Adaptive Neuron Control Using an Integrated Error Approach with Application to Active Suspensions", *International Journal of Automotive Technology*, Vol. 9, No. 3, pp. 329 - 335, June 2008.

[31] I. Eski and S. Yildrim: "Vibration Control of Vehicle Active Suspension System Using a New Robust Neural Network Control System", *Simulation Modelling Practice and Theory*, Vol. 17, No. 5, pp. 778 - 793, May 2009.

[32] K. Valarmathi, D. Devaraj and T. K. Radhakrishnan: "Intelligent Techniques for System Identification and Controller Tuning in pH Process", *Brazilian Journal of Chemical Engineering*, Vol. 26, No. 1, pp. 99 - 111, January - March 2009.

[33] M. Jelali and A. Kroll: "Hydraulic Servo-Systems: Modelling, Identification and Control", *Springer*, London, 2003.

[34] H. Demuth and M. Beale: "Neural Networks Toolbox User's Guide: For use with MATLAB", *The MathWorks, Inc*, Massachusetts, 2002.

[35] F. S. Mjalli and S. Al-Asheh: "Neural-Networks-Based Feedback Linearization versus Model Predictive Control of Continuous Alcoholic Fermentation Process", *Chemical Engineering Technology*, Vol. 28, No. 10, pp. 1191 - 1120, October 2005.

[36] K. K. Ahn, H. P. H. Ahn and N. T. Kiet: "A Comparative Study of Modelling and Identification of the Pneumatic Artificial Muscle (PAM) Manipulator based on Recurrent Neural Networks", *Proceedings of the International Symposium on Electrical and Electronics Engineering*, HCM city, Vietnam, 2007.

[37] Q. Zhang and L. Ljung: "Multiple Steps Prediction with nonlinear ARX Models", *Proceedings of the Symposium on nonlinear Control Systems (NOLCOS)*, Stuttgart, Germany, 2004.

[38] M. H. F. Rahiman, M. N. Taib and Y. M. Salleh: "Selection of Training Data for Modelling Essential Oil Extraction System using NNARX Structure", *Proceedings of the International Conference on Control, Automation and Systems*, Seoul, Korea, 2007.

[39] M. T. Hagan, H. B. Demuth and O. Jesus: "An Introduction to the use of Neural Networks in Control Systems", *International Journal of Robust and nonlinear Control*, Vol. 12, No. 11, pp. 959 - 985, September 2002.

[40] S. Haykin, S: "Neural Networks and Learning Machines", Pearson Education, Inc, New Jersey, 2009.

[41] J. Žilková, J. Timko and P. Girovský: "Nonlinear System Control Using Neural Networks", *Acta Polytechnica Hungrica*, Budapest, Hungary, 2006.

[42] A. O'Dwyer: "Handbook of PI and PID Controller Tuning Rules", Imperial College Press, London, 2006.